

Polynomial Preserving Recovery for High Frequency Wave Propagation

Hailong Guo¹  · Xu Yang¹

Received: 7 March 2016 / Revised: 16 August 2016 / Accepted: 20 October 2016 /
Published online: 25 October 2016
© Springer Science+Business Media New York 2016

Abstract Polynomial preserving recovery (PPR) was first proposed and analyzed in Zhang and Naga in *SIAM J Sci Comput* 26(4):1192–1213, (2005), with intensive following applications on elliptic problems. In this paper, we generalize the study of PPR to high-frequency wave propagation. Specifically, we establish the supercloseness between finite element solution and its interpolation with explicit dependence on the frequency of wavefield, and then prove the superconvergence of PPR for high-frequency solutions to wave equation based on the supercloseness. We also present several numerical examples of PPR for both low-frequency and high-frequency wave propagation in order to confirm the theoretical results of superconvergence analysis.

Keywords Wave equation · High-frequency · Polynomial preserving · Gradient recovery · Superconvergence · Finite element method

Mathematics Subject Classification Primary 65N50 · 65N30; Secondary 65N15

1 Introduction

Superconvergence has been one of the important research topics in the community of finite element methods; see [36] and references therein. In general, it can be classified into two categories: natural superconvergence (e.g. [8, 13, 14]) and postprocessing superconvergence (e.g.

This work was partially supported by the NSF Grants DMS-1418936 and DMS-1107291, and Hellman Family Foundation Faculty Fellowship, UC Santa Barbara. We also acknowledge support from the Center for Scientific Computing from the CNSI, MRL: an NSF MRSEC (DMR-1121053) and NSF CNS-0960316.

✉ Hailong Guo
hlguo@math.ucsb.edu

Xu Yang
xuyang@math.ucsb.edu

¹ Department of Mathematics, University of California, Santa Barbara, CA 93106, USA

[20,25,30,31,39,44–47]). One of the major postprocessing techniques is gradient recovery methods, which are able to provide asymptotically exact a posteriori error estimators [1,2,7,30,45–47], anisotropical mesh adaption [18,19,22], and enhancement of eigenvalue approximation [21,32,40]. A famous example of gradient recovery methods is the Superconvergent Patch Recovery (SPR) proposed by Zienkiewicz and Zhu [46], also known as ZZ estimator, which has become a standard tool in many commercial Finite Element softwares such as ANSYS, Abaqus, and LS-DYNA. An important alternative is the polynomial preserving recovery (PPR) proposed by Zhang and Naga [44], which improved the performance of SPR on chevron pattern uniform mesh. It has also been implemented by commercial Finite Element software COMSOL Multiphysics as a superconvergence tool. Nevertheless, studies of both SPR and PPR have been mostly focused on elliptic problems.

Study on superconvergence of second order hyperbolic equations can be traced back to [15] where Dougalis and Serbin proved finite element solution was superconvergent to a special quasi-interpolation of exact solution in one-dimension. Later on, Lin et al. [28] investigated an interpolated finite element solution for bilinear element and showed it has superconvergence. Analogous to [28], Shi and Li [34] studied the superconvergence for a nonlinear second order hyperbolic equation with nonlinear boundary conditions. Recent works include [37], where Wang et al. showed the superconvergence of mixed finite element solution to full discrete wave equations. In [3], Baccouch justified that the local discontinuous Galerkin solution superconverges at Radau points on Cartesian grids. In [12], Cockburn et al. used hybridizable discontinuous Galerkin methods to solve wave equation and got a uniform-in-time superconvergence result.

In this paper, we generalize the polynomial preserving recovery (PPR) technique to study high-frequency wave propagation, governed by a second order hyperbolic equation. First, we establish the supercloseness between finite element solution and its interpolation with explicit dependence on wave frequency. Our main tool is the superconvergence of interpolation solution of linear element [5,9,42] and quadratic element [23] in the weak sense. Generalizing PPR from elliptic equations to hyperbolic equations leads to a difficulty that the superconvergence arguments for elliptic problems, relying on maximal norm of higher order weak derivative, do not hold for hyperbolic equations due to the loss of maximal principle [5,9,23,42]. To overcome the difficulty, we need to put more restrictions on the mesh in order to compensate the loss of order of errors caused by solution regularities. Specifically, we require the mesh to satisfy *Condition* (α), i.e. any two adjacent triangles form an $O(h^{1+\alpha})$ parallelogram, with a more detailed explanation given in Sect. 2. We also remark that this mesh restriction is just for theoretical purpose, but not for numerical simulations as shown by our later examples in Sect. 5.

The superconvergence of PPR for wave equation follows the standard procedure in [1] that decomposes the error into two parts. The first part can be bounded by the aforementioned supercloseness results thanking to the boundedness of PPR gradient recovery operator. The second part is usually bounded by consistency of gradient recovery operator. However, such type of error estimate, e.g. in [30,31,44], is not sharp for hyperbolic problems since it involves with the infinity Sobolev norm. In fact, we use the polynomial preserving property of PPR and scaled Bramble–Hilbert Lemma to establish a sharp bound that only involves with the L^2 Sobolev norm. We remark that the sharp bound actually works for any arbitrary order of element, although we only consider linear element and quadratic element in this paper.

The rest of the paper is organized as follows. Section 2 introduces preliminaries on wave equation and the finite element approximation. In Sect. 3, we analyze the supercloseness between finite element solution and the interpolation of exact solution, and give explicit dependence of the estimate on wave frequency. Section 4 is devoted to the proof of supercon-

vergence of PPR. We present several numerical examples to confirm our theoretical results in Sect. 5, and make conclusive remarks in Sect. 6.

2 Wave Equation and Finite Element Approximation

We shall consider the following linear wave equation

$$\frac{\partial^2 u}{\partial t^2}(x, t) - \nabla \cdot (\Sigma(x)\nabla u(x, t)) = f(x, t), \quad (x, t) \in \Omega \times (0, T], \tag{2.1a}$$

$$u(x, t) = 0, \quad (x, t) \in \partial\Omega \times (0, T], \tag{2.1b}$$

$$u(x, 0) = u_0(x), \quad x \in \Omega, \tag{2.1c}$$

$$\frac{\partial u}{\partial t}(x, 0) = q_0(x), \quad x \in \Omega, \tag{2.1d}$$

with the following WKB initial conditions, for $k \gg 1$,

$$u_0(x) = A_0(x)e^{ikS_0(x)}, \tag{2.2a}$$

$$q_0(x) = kB_0(x)e^{ikS_0(x)}. \tag{2.2b}$$

Here Ω is a bounded polygonal domain with Lipschitz boundary $\partial\Omega$ in \mathbb{R}^2 , f, A_0, B_0, S_0 are given functions, and $\Sigma(x)$ is a 2×2 symmetric positive definite matrix valued function. $k \gg 1$ indicates the wave is of high-frequency.

Computing high-frequency wave propagation (2.1)–(2.2) is an important problem arising in many applications including electromagnetic radiation and scattering, seismic and acoustic waves traveling. There coexists two scales when $k \gg 1$ in (2.2): The large length scale is determined by the characteristic size of Ω , while the small length scale comes from the wavelength at the order of $O(k^{-1})$. The disparity between the two length scales makes direct numerical computations extremely challenging, which motivates us to study the polynomial preserving recovery method for (2.1)–(2.2).

Notations We use C to denote a generic positive constant which may be different at different occurrences. For a sake of simplicity, we use $x \lesssim y$ to mean that $x \leq Cy$ for some constants C independent of mesh size and frequency of wavefield. For a subdomain \mathcal{A} of Ω , denote $W^{k,p}(\mathcal{A})$ as the Sobolev space with norm $\|\cdot\|_{k,p,\mathcal{A}}$ and seminorm $|\cdot|_{k,p,\mathcal{A}}$. We also denote $H^k(\mathcal{A}) = W^{k,2}(\mathcal{A})$. These are the standard notations for Sobolev spaces and their associate norms in [6, 11].

Following the same notations in [4, 29], for $v : [0, T] \rightarrow H$ Lebesgue measurable, we define the following norms

$$\|v\|_{L^2(0,T;W^{k,p}(\Omega))} = \left(\int_0^T \|v(\cdot, t)\|_{k,p,\Omega}^2 dt \right)^{1/2}, \tag{2.3}$$

and

$$\|v\|_{L^\infty(0,T;W^{k,p}(\Omega))} = \operatorname{ess\,sup}_{0 \leq t \leq T} \|v(\cdot, t)\|_{k,p,\Omega}. \tag{2.4}$$

In addition, we define

$$L^q(0, T; W^{k,p}(\Omega)) = \{v : [0, T] \rightarrow W^{k,p}(\Omega) : \|v\|_{L^q(0,T;W^{k,p}(\Omega))} < \infty\}, \tag{2.5}$$

where $q = 2, \infty$.

For wave equation (2.1), the following regularity estimate was provided in [17].

Theorem 2.1 Assume $u_0 \in H^{m+1}(\Omega)$, $q_0 \in H^m(\Omega)$, and $\frac{d^\ell f}{dt^\ell} \in L^2(0, T; H^{m-\ell}(\Omega))$. Then

$$\frac{d^\ell u}{dt^\ell} \in L^\infty(0, T; H^{m+1-\ell}(\Omega)), \quad (\ell = 0, \dots, m + 1), \tag{2.6}$$

and we have the following estimate

$$\begin{aligned} & \operatorname{ess\,sup}_{0 \leq t \leq T} \sum_{\ell=0}^{m+1} \left\| \frac{d^\ell u}{dt^\ell} \right\|_{H^{m+1-\ell}(\Omega)} \\ & \leq C \left(\sum_{\ell=0}^m \left\| \frac{d^\ell f}{dt^\ell} \right\|_{L^2(0, T; H^{m-\ell}(\Omega))} + \|u_0\|_{m+1, \Omega} + \|q_0\|_{m, \Omega} \right). \end{aligned} \tag{2.7}$$

In particular, for wave equation (2.1) with WKB initial conditions (2.2), Theorem 2.1 implies the following regularity estimate with explicit dependence on k .

Theorem 2.2 Assume the same condition as in Theorem 2.1 holds. Let u be solution of wave equation (2.1a)–(2.1b) with the following WKB initial conditions (2.2a)–(2.2b). Then we have

$$\left\| \frac{d^\ell u}{dt^\ell} \right\|_{L^\infty(0, T; H^{m+1-\ell}(\Omega))} \leq Ck^{m+1}, \tag{2.8}$$

where C is a number independent of k .

Define the sesquilinear form $a(\cdot, \cdot)$ as

$$a(u, v) = \int_{\Omega} \nabla u \cdot \Sigma \nabla \bar{v} dx, \quad \forall u, v \in H^1(\Omega), \tag{2.9}$$

where \bar{v} is the complex conjugate of v . Then one can see that $a(\cdot, \cdot)$ is a continuous and coercive bilinear form defined on $H_0^1(\Omega)$. In addition, we define the norm

$$\| \cdot \|_{a, \Omega} = \sqrt{a(\cdot, \cdot)}, \tag{2.10}$$

which can be easily verified to be equivalent to $| \cdot |_{1, \Omega}$ on $H_0^1(\Omega)$.

The weak formulation of (2.1) is to find $u \in L^2(0, T; H_0^1(\Omega))$ with $\frac{\partial^2 u}{\partial t^2} \in L^2(0, T; H^{-1}(\Omega))$ such that

$$\left(\frac{\partial^2}{\partial t^2} u(\cdot, t), v \right) + a(u(\cdot, t), v) = (f(\cdot, t), v), \quad \forall v \in H_0^1(\Omega), t \in (0, T], \tag{2.11}$$

and

$$u(x, 0) = u_0, \quad x \in \Omega, \tag{2.12}$$

$$\frac{\partial u}{\partial t}(x, 0) = q_0, \quad x \in \Omega. \tag{2.13}$$

The existence and uniqueness of the solution to (2.11)–(2.13) were established in [29] for $f \in L^2(0, T; H^{-1}(\Omega))$ and $u_0, q_0 \in H_0^1(\Omega)$.

Let \mathcal{T}_h be a conforming triangulation of the domain Ω , and consists of triangles T with diameter $h_T \leq h$. Furthermore, we assume \mathcal{T}_h is shape-regular in the sense of [11]. The triangulation \mathcal{T}_h is called to satisfy *Condition* (α) if there exists $\alpha > 0$ such that any two adjacent triangles form an $O(h^{1+\alpha})$ parallelogram, which means for any two adjacent triangles (sharing a common edge), the lengths of any two opposite edges differ only by $O(h^{1+\alpha})$.

Define the continuous finite element space of order r as

$$S^{h,r} = \{v \in C(\bar{\Omega}) : v|_T \in \mathbb{P}_r(T), \forall T \in \mathcal{T}_h\} \subset H^1(\Omega),$$

where $\mathbb{P}_r(T)$ is the space of polynomials of degree less than or equal to r over T . The set of nodal point in $S^{h,r}$ is denote by \mathcal{N}_h . Also, we denote $S_0^{h,r} = S^{h,r} \cap H_0^1(\Omega)$, and $I_h^r u$ to be the standard Lagrange interpolation of polynomial of order r in the finite element space $S^{h,r}$. Then the continuous-time Galerkin approximation to (2.11)–(2.13) reads as, to find $u_h \in L^2(0, T; S_0^{h,r})$ such that,

$$\left(\frac{\partial^2 u_h}{\partial t^2}(\cdot, t), v\right) + a(u_h(\cdot, t), v) = (f(\cdot, t), v), \tag{2.14}$$

for any $v \in S_0^{h,r}$ and $t \in (0, T]$ with

$$u_h(\cdot, 0) = I_h^r u_0, \tag{2.15}$$

$$\frac{\partial u_h}{\partial t}(\cdot, 0) = I_h^r q_0. \tag{2.16}$$

For the approximation (2.14)–(2.16), one can have the following error estimate [4, 16].

Theorem 2.3 *Let u_h be the solution of (2.14)–(2.16). Suppose $u \in L^\infty(0, T; H^{r+1}(\Omega))$ and $\frac{\partial u}{\partial t} \in L^2(0, T; H^{r+1}(\Omega))$, then we have*

$$\begin{aligned} & \|u - u_h\|_{L^\infty(0,T;L^2(\Omega))} + h\|u - u_h\|_{L^\infty(0,T;H^1(\Omega))} \\ & \lesssim h^{r+1} \left(\|u\|_{L^\infty(0,T;H^{r+1}(\Omega))} + \left\| \frac{\partial u}{\partial t} \right\|_{L^2(0,T;H^{r+1}(\Omega))} \right) \\ & \lesssim (hk)^{r+1} + k(hk)^{r+1} \\ & \lesssim k(hk)^{r+1}, \end{aligned} \tag{2.17}$$

where the last inequality is due to $k \gg 1$.

Remark 2.4 The H^1 -semi error in Theorem 2.3 consists of two parts: the first term $k(hk)^r$ can be regarded as interpolation error of u

$$\|\nabla u - \nabla I_h^r u\|_{0,\Omega} \leq h^r |u|_{r+1,\Omega} \leq h^r k^{r+1},$$

while the second term $k^2(hk)^r$ is due to the interpolation error of $\frac{\partial u}{\partial t}$,

$$\left\| \nabla \frac{\partial u}{\partial t} - \nabla I_h^r \frac{\partial u}{\partial t} \right\|_{0,\Omega} \leq h^r \left| \frac{\partial u}{\partial t} \right|_{r+1,\Omega} \leq h^r k^{r+2}.$$

This is different from finite element approximation of Helmholtz equation [26, 27, 38].

Remark 2.5 Theorem 2.3 indicates the mesh size h should be of $O(k^{-3})$ to give an accurate approximation to high-frequency propagation by linear element, but this estimate may not be sharp, as shown later by our numerical results in Sect. 5.

3 Supercloseness of Finite Element Solution

In this section, we establish the supercloseness between finite element solution and the interpolation of the exact solution for both linear element and quadratic element.

Lemma 3.1 Assume \mathcal{T}_h satisfies Condition (α) . Let Σ_τ be a piecewise constant matrix function defined on \mathcal{T}_h , whose elements $\Sigma_{\tau ij}$ satisfy

$$\Sigma_{\tau ij} \lesssim 1, \quad |\Sigma_{\tau ij} - \Sigma_{\tau' ij}| \leq h^\alpha, \quad i = 1, 2; j = 1, 2. \tag{3.1}$$

Here τ and τ' are a pair of triangles sharing a common edge. In addition, suppose $u \in H_0^1(\Omega) \cap H^{2+r}(\Omega)$, then for any $v_h \in S_0^{h,r}$,

$$\left| \sum_{\tau \in \mathcal{T}_h} \int_{\tau} \nabla(u - I_h^r u) \cdot \Sigma_\tau \nabla v_h \right| \lesssim h^{r+\alpha} \|u\|_{r+2, \Omega} \|v\|_{1, \Omega}, \tag{3.2}$$

where $r = 1, 2$.

Proof For the linear element case, the proof is similar to Lemma 2.1 in [42]. For the quadratic element case, one can prove it by modifying the proof of Theorem 4.3 in [23]. \square

Remark 3.2 It is worth mentioning that the mesh condition is more restrictive than that in [5, 9, 42] for linear element, due to the lack of $|u|_{2, \infty}$ estimate for wave equation. Note that this restriction is technique and just for theoretical purpose. In fact, numerical experiments in Sect. 5 indicate that one can still get results of superconvergence under general Delaunay meshes which do not satisfy the Condition (α) .

We define the constant matrix function Σ_τ in term of the diffusion coefficient matrix Σ in (2.1a) as follows

$$\Sigma_{\tau ij} = \frac{1}{|\tau|} \int_{\tau} \Sigma_{ij} dx, \tag{3.3}$$

for $i, j = 1, 2$. We assume Σ is smooth enough so that the condition (3.1) in Lemma 3.1 holds and the following inequality is also true,

$$|\Sigma - \Sigma_\tau| \lesssim h, \quad \forall \tau \in \mathcal{T}_h. \tag{3.4}$$

Subtracting (2.11) from (2.14) implies that, for any $v \in S_0^{h,r}$,

$$\left(\frac{\partial^2}{\partial t^2} u_h - \frac{\partial^2}{\partial t^2} u, v \right) + a(u_h - u, v) = 0, \tag{3.5}$$

and one can prove the following supercloseness result.

Theorem 3.3 Let u be exact solution to the wave equation (2.11) and u_h be solution of the semi-discrete Galerkin finite element approximation (2.14). Assume the mesh \mathcal{T}_h satisfies Condition (α) , and $u \in L^\infty(0, T; H^{r+2}(\Omega))$, $\frac{\partial u}{\partial t} \in L^2(0, T; H^{r+2}(\Omega))$, and $\frac{\partial^2 u}{\partial t^2} \in L^2(0, T; H^{r+1}(\Omega))$, then we have

$$\|u_h(\cdot, t) - I_h^r u(\cdot, t)\|_{1, \Omega} \leq Ch^{r+\min(1, \alpha)} k^{r+3}, \tag{3.6}$$

where C is a constant independent of k and h .

Proof Denote $\eta = u_h - I_h^r u$ and $\xi = u - I_h^r u$, then (3.5) implies that

$$\left(\frac{\partial^2}{\partial t^2} \eta, v \right) + a(\eta, v) = \left(\frac{\partial^2}{\partial t^2} \xi, v \right) + a(\xi, v), \tag{3.7}$$

for any $v \in S_0^{r,h}$. Taking $v = \frac{\partial \eta}{\partial t}$ brings

$$\left(\frac{\partial^2}{\partial t^2} \eta, \frac{\partial \eta}{\partial t} \right) + a \left(\eta, \frac{\partial \eta}{\partial t} \right) = \left(\frac{\partial^2}{\partial t^2} \xi, \frac{\partial \eta}{\partial t} \right) + a \left(\xi, \frac{\partial \eta}{\partial t} \right), \tag{3.8}$$

which can be rewritten as

$$\frac{1}{2} \frac{\partial}{\partial t} \left(\frac{\partial \eta}{\partial t}, \frac{\partial \eta}{\partial t} \right) + \frac{1}{2} \frac{\partial}{\partial t} a(\eta, \eta) = \left(\frac{\partial^2}{\partial t^2} \xi, \frac{\partial \eta}{\partial t} \right) + a \left(\xi, \frac{\partial \eta}{\partial t} \right). \tag{3.9}$$

Integrating (3.9) with respect to t from 0 to s produces

$$\begin{aligned} & \frac{1}{2} \left\| \frac{\partial}{\partial t} \eta(\cdot, s) \right\|_{0,\Omega}^2 + \frac{1}{2} a(\eta(\cdot, s), \eta(\cdot, s)) \\ &= \int_0^s \left(\frac{\partial^2}{\partial t^2} \xi(\cdot, t), \frac{\partial \eta(\cdot, t)}{\partial t} \right) dt + \int_0^s a \left(\xi(\cdot, t), \frac{\partial \eta(\cdot, t)}{\partial t} \right) dt \\ &= \int_0^s \left(\frac{\partial^2}{\partial t^2} \xi(\cdot, t), \frac{\partial \eta(\cdot, t)}{\partial t} \right) dt + a(\xi(\cdot, s), \eta(\cdot, s)) - \int_0^s a \left(\frac{\partial \xi(\cdot, t)}{\partial t}, \eta(\cdot, t) \right) dt \\ &= \int_0^s \left(\frac{\partial^2}{\partial t^2} \xi(\cdot, t), \frac{\partial \eta(\cdot, t)}{\partial t} \right) dt + \sum_{\tau \in \mathcal{T}_h} \int_{\tau} \nabla \xi(\cdot, t) \cdot \Sigma_{\tau} \nabla \overline{\eta(\cdot, t)} \\ &\quad - \sum_{\tau \in \mathcal{T}_h} \int_{\tau} \nabla \xi(\cdot, t) \cdot (\Sigma_{\tau} - \Sigma) \nabla \overline{\eta(\cdot, t)} - \int_0^s \left(\sum_{\tau \in \mathcal{T}_h} \int_{\tau} \nabla \frac{\partial \xi(\cdot, t)}{\partial t} \cdot \Sigma_{\tau} \nabla \overline{\eta(\cdot, t)} \right) dt \\ &\quad + \int_0^s \left(\sum_{\tau \in \mathcal{T}_h} \int_{\tau} \nabla \frac{\partial \xi(\cdot, t)}{\partial t} \cdot (\Sigma_{\tau} - \Sigma) \nabla \overline{\eta(\cdot, t)} \right) dt \\ &=: I_1 + I_2 + I_3 + I_4 + I_5, \end{aligned}$$

where we have used the fact $\eta(\cdot, 0) = \frac{\partial \eta}{\partial t}(\cdot, 0) = 0$, i.e. (2.15) and (2.16).

We first estimate I_1 . By Hölder’s inequality and Cauchy’s inequality, one has

$$\begin{aligned} I_1 &\leq \int_0^s \left\| \frac{\partial^2}{\partial t^2} \xi(\cdot, t) \right\|_{0,\Omega} \left\| \frac{\partial}{\partial t} \eta(\cdot, t) \right\|_{0,\Omega} dt \\ &\leq C \int_0^s \left\| \frac{\partial^2}{\partial t^2} \xi(\cdot, t) \right\|_{0,\Omega}^2 dt + \int_0^s \left\| \frac{\partial}{\partial t} \eta(\cdot, t) \right\|_{0,\Omega}^2 dt \\ &\leq Ch^{2r+2} \left\| \frac{\partial^2}{\partial t^2} u \right\|_{L^2(0,T;H^{r+1}(\Omega))}^2 + \int_0^s \left\| \frac{\partial}{\partial t} \eta(\cdot, t) \right\|_{0,\Omega}^2 dt, \end{aligned} \tag{3.10}$$

where we have used the standard L_2 norm error estimation of finite element interpolation $I_h^r u$ [6, 11]. Lemma 3.1 implies that

$$I_2 \leq Ch^{r+\alpha} \|u(\cdot, s)\|_{r+2,\Omega} |\eta(\cdot, s)|_{1,\Omega} \leq Ch^{2r+2\alpha} \|u(\cdot, s)\|_{r+2,\Omega}^2 + \frac{1}{8} \|\eta(\cdot, s)\|_{a,\Omega}^2. \tag{3.11}$$

I_3 is estimated by

$$\begin{aligned} I_3 &\leq \sum_{\tau \in \mathcal{T}_h} \int_{\tau} |\nabla \xi(\cdot, t)| |(\Sigma_{\tau} - \Sigma)| |\nabla \xi(\cdot, s)| \\ &\leq h |\xi(\cdot, s)|_{1,\Omega} |\eta(\cdot, s)|_{1,\Omega} \\ &\leq Ch^{r+1} \|u\|_{r+1,\Omega} |\eta(\cdot, s)|_{1,\Omega} \\ &\leq Ch^{2r+2} \|u(\cdot, s)\|_{r+1,\Omega}^2 + \frac{1}{8} \|\eta(\cdot, s)\|_{a,\Omega}^2, \end{aligned} \tag{3.12}$$

where the third inequality comes from the standard H_1 interpolation error estimate [6, 11]. For I_4 , Lemma 3.1 implies

$$\begin{aligned}
 I_4 &\leq \int_0^s h^{r+\alpha} \left\| \frac{\partial u}{\partial t}(\cdot, s) \right\|_{r+2, \Omega} |\eta(\cdot, s)|_{1, \Omega} dt \\
 &\leq Ch^{2r+2\alpha} \left\| \frac{\partial u}{\partial t} \right\|_{L^2(0, T; H^{r+2}(\Omega))}^2 + \int_0^s \|\eta(\cdot, t)\|_{a, \Omega}^2 dt.
 \end{aligned}
 \tag{3.13}$$

Similarly, we can get the following estimate of I_5

$$\begin{aligned}
 I_5 &\leq \int_0^s Ch^{r+1} \left\| \frac{\partial u}{\partial t}(\cdot, s) \right\|_{r+1, \Omega} |\eta(\cdot, s)|_{1, \Omega} dt \\
 &\leq Ch^{2r+2} \left\| \frac{\partial u}{\partial t} \right\|_{L^2(0, T; H^{r+1}(\Omega))}^2 + \int_0^s \|\eta(\cdot, t)\|_{a, \Omega}^2 dt.
 \end{aligned}
 \tag{3.14}$$

Combining the error estimates (3.10)–(3.14) gives

$$\begin{aligned}
 &\frac{1}{2} \left\| \frac{\partial}{\partial t} \eta(\cdot, s) \right\|_{0, \Omega}^2 + \frac{1}{8} \|\eta(\cdot, s)\|_{a, \Omega}^2 \\
 &\leq Ch^{2r+2} \left\| \frac{\partial^2 u}{\partial t^2} \right\|_{L^2(0, T; H^{r+1}(\Omega))}^2 + Ch^{2r+2\alpha} \left\| \frac{\partial u}{\partial t} \right\|_{L^2(0, T; H^{r+2}(\Omega))}^2 \\
 &\quad Ch^{2r+2\alpha} \|u(\cdot, s)\|_{r+2, \Omega}^2 + Ch^{2r+2} \|u(\cdot, s)\|_{r+1, \Omega}^2 \\
 &\quad + Ch^{2r+2} \left\| \frac{\partial^2 u}{\partial t^2} \right\|_{L^2(0, T; H^{r+1}(\Omega))}^2 + \int_0^s \left\| \frac{\partial}{\partial t} \eta(\cdot, t) \right\|_{0, \Omega}^2 dt \\
 &\quad + 2 \int_0^s \|\eta(\cdot, t)\|_{a, \Omega}^2 dt,
 \end{aligned}
 \tag{3.15}$$

and thus Gronwall’s inequality [17] produces

$$\begin{aligned}
 &\left\| \frac{\partial}{\partial t} \eta(\cdot, s) \right\|_{0, \Omega}^2 + \|\eta(\cdot, s)\|_{a, \Omega}^2 \\
 &\leq Ch^{2r+2} \left\| \frac{\partial^2 u}{\partial t^2} \right\|_{L^2(0, T; H^{r+1}(\Omega))}^2 + Ch^{2r+2} \left\| \frac{\partial u}{\partial t} \right\|_{L^2(0, T; H^{r+1}(\Omega))}^2 \\
 &\quad + Ch^{2r+2\alpha} \left\| \frac{\partial u}{\partial t} \right\|_{L^2(0, T; H^{r+2}(\Omega))}^2 + Ch^{2r+2\alpha} \|u(\cdot, s)\|_{r+2, \Omega}^2 \\
 &\quad + Ch^{2r+2} \|u(\cdot, s)\|_{r+1, \Omega}^2.
 \end{aligned}$$

In particular, we have, for any $0 \leq s \leq T$,

$$|\eta(\cdot, s)|_{1, \Omega} \leq C \left(h^{r+\min(1, \alpha)} k^{r+3} + h^{r+\min(1, \alpha)} k^{r+1} \right) \leq Ch^{r+\min(1, \alpha)} k^{r+3},$$

where we have used the fact that $k \gg 1$ in the last inequality. Replacing s by t completes our proof. □

Remark 3.4 Using the standard argument instead of superconvergence argument will give the following error estimate for $\|\nabla u_h - \nabla I_h^r u\|_{0, \Omega}$,

$$\|\nabla u_h - \nabla I_h^r u\|_{0, \Omega} \lesssim h^r k^{r+2}.
 \tag{3.16}$$

Remark 3.5 Numerical examples later in Sect. 5 indicate that $\|\nabla u_h - \nabla I_h^r u\|_{0,\Omega} \lesssim h^2$ and $\|\nabla u_h - \nabla I_h^r u\|_{0,\Omega} \lesssim k^3$ for linear element, which means the error estimates (3.6) and (3.16) are not sharp with respect to k and h respectively.

4 Superconvergence of Polynomial Preserving Recovery

In this section, we analyze the superconvergence of polynomial preserving recovery (PPR) for wave equation (2.1). Denote the PPR gradient recovery operator by G_h , then G_h is a linear operator from $S^{h,r}$ to $S^{h,r} \times S^{h,r}$. Given a function $u_h \in S_h^r$, it suffices to define $(G_h u_h)(z)$ for all $z \in \mathcal{N}_h$. Let $z \in \mathcal{N}_h$ be a vertex and \mathcal{K}_z be a patch of elements around z which is defined in [31,44]. Select all nodes in $\mathcal{N}_h \cap \mathcal{K}_z$ as sampling points and fit a polynomial $p_z \in \mathbb{P}_{k+1}(\mathcal{K}_z)$ in the least squares sense at those sampling points, i.e.

$$p_z = \arg \min_{p \in \mathbb{P}_{k+1}(\mathcal{K}_z)} \sum_{\tilde{z} \in \mathcal{N}_h \cap \mathcal{K}_z} (u_h - p)^2(\tilde{z}). \tag{4.1}$$

Then the recovered gradient at z is defined as

$$(G_h u_h)(z) = \nabla p_z(z).$$

For linear element, all nodes in \mathcal{N}_h are vertices and hence $G_h u_h$ is well defined. However, \mathcal{N}_h may contain edge nodes or interior nodes for higher order elements. If z is an edge node which lies on an edge between two vertices z_1 and z_2 , we define

$$(G_h u_h)(z) = \beta \nabla p_{z_1}(z) + (1 - \beta) \nabla p_{z_2}(z)$$

where β is determined by the ratio of distances of z to z_1 and z_2 . If z is an interior node which lies in a triangle formed by three vertices z_1, z_2 , and z_3 , we define

$$(G_h u_h)(z) = \sum_{j=1}^3 \beta_j \nabla p_{z_j}(z),$$

where β_j is the barycentric coordinate of z .

Remark 4.1 It was proved in [30] that certain rank condition and geometric condition guarantee the uniqueness of p_z in (4.1).

Remark 4.2 In order to avoid numerical instability, a discrete least squares fitting process is carried out on a reference patch ω_z .

For the PPR gradient recovery operator G_h , [30,31,44] proved that G_h has the following properties:

- (i) G_h preserves polynomials of degree $r + 1$.
- (ii) $\|G_h v\|_{0,\tau} \lesssim |v|_{1,\mathcal{K}_\tau}, \forall \tau \in \mathcal{T}_h$, where $\mathcal{K}_\tau := \bigcup \{\mathcal{K}_z : z \text{ is a vertex of } \tau\}$.
- (iii) $\|\nabla u - G_h u\|_{0,\infty,\mathcal{K}_z} \leq Ch^{r+1} |u|_{r+2,\infty,\mathcal{K}_z}$.

Note that in Property (iii), $\|\nabla u - G_h u\|_{0,\infty,\mathcal{K}_z}$ is bounded by the $W^{r+2,\infty}$ norm of the exact solution u . However, such regularity is not available for wave equation (2.1). In the following, we shall prove a sharp type error estimate analogous to property (iii).

According to Property (i) of G_h , we can prove the following lemma.

Lemma 4.3 Let $G_h : S^{h,r} \rightarrow S^{h,r} \times S^{h,r}$ be the PPR gradient recovery operator. Given $u \in H^{r+2}(\Omega)$, then

$$\|G_h I_h^r u - \nabla u\|_{0,\tau} \lesssim h^{r+1} \|u\|_{r+2,\mathcal{K}_\tau}, \tag{4.2}$$

for any $\tau \in \mathcal{T}_h$.

Proof Notice that

$$\begin{aligned} \|G_h I_h^r u - \nabla u\|_{0,\tau} &\leq \|G_h I_h^r u - G_h I_h^r I_h^{r+1} u\|_{0,\tau} + \|G_h I_h^r I_h^{r+1} u - \nabla u\|_{0,\tau} \\ &= \|G_h I_h^r u - G_h I_h^r I_h^{r+1} u\|_{0,\tau} + \|G_h I_h^{r+1} u - \nabla u\|_{0,\tau} \\ &:= I_1 + I_2, \end{aligned} \tag{4.3}$$

where we have used the fact that $G_h I_h^r I_h^{r+1} u = G_h I_h^{r+1} u$ since we only use nodal points in the recovery operator G_h . We begin with the estimate of I_2 . According to Property (i), we have $G_h I_h^r v = \nabla v$ for any $v \in \mathbb{P}_{r+1}(\mathcal{K}_\tau)$, which implies that

$$\begin{aligned} I_2 &= \|G_h(I_h^{r+1} u - v) - \nabla(u - v)\|_{0,\tau} \\ &\leq \|G_h(I_h^{r+1} u - v)\|_{0,\tau} + \|\nabla(u - v)\|_{0,\tau} \\ &\lesssim \|\nabla(I_h^{r+1} u - v)\|_{0,\mathcal{K}_\tau} + \|\nabla(u - v)\|_{0,\tau} \\ &\lesssim \|\nabla(I_h^{r+1} u - u)\|_{0,\mathcal{K}_\tau} + \|\nabla(u - v)\|_{0,\mathcal{K}_\tau} + \|\nabla(u - v)\|_{0,\tau} \\ &\lesssim \|\nabla(I_h^{r+1} u - u)\|_{0,\mathcal{K}_\tau} + \|\nabla(u - v)\|_{0,\mathcal{K}_\tau}. \end{aligned} \tag{4.4}$$

Standard approximation theory of finite element [6, 11] implies

$$\|\nabla(I_h^{r+1} u - u)\|_{0,\mathcal{K}_\tau} \lesssim h^{r+1} \|u\|_{r+2,\mathcal{K}_\tau}. \tag{4.5}$$

Let $F(u) = \inf_{v \in \mathbb{P}_{r+1}(\mathcal{K}_\tau)} \|\nabla(u - v)\|_{0,\mathcal{K}_\tau}$, then it is easy to see $F(v) = 0$ for any $v \in \mathbb{P}_{r+1}(\mathcal{K}_\tau)$.

By Bramble–Hilbert lemma, one has

$$\|\nabla(u - v)\|_{0,\mathcal{K}_\tau} \leq h^{r+1} \|u\|_{r+2,\mathcal{K}_\tau}. \tag{4.6}$$

Now, we turn to estimate I_1 . The boundedness of G_h implies

$$I_1 = \|G_h I_h^r u - G_h I_h^r I_h^{r+1} u\|_{0,\tau} \lesssim \|\nabla(I_h^r u - I_h^r I_h^{r+1} u)\|_{0,\mathcal{K}_\tau}. \tag{4.7}$$

Notice that $I_h^{r+1} v = v$ and hence $I_h^r v = I_h^r I_h^{r+1} v$ for all $v \in \mathbb{P}_{r+1}(\mathcal{K}_\tau)$. Define $\tilde{F} = \|\nabla(I_h^r u - I_h^r I_h^{r+1} u)\|_{0,\mathcal{K}_\tau}$. Then it is easy to see that $\tilde{F}(v) = 0$ for any $v \in \mathbb{P}_{r+1}(\mathcal{K}_\tau)$. Again Bramble–Hilbert lemma suggests that

$$\|\nabla(I_h^r u - I_h^r I_h^{r+1} u)\|_{0,\mathcal{K}_\tau} \lesssim h^{r+1} \|u\|_{r+2,\mathcal{K}_\tau}. \tag{4.8}$$

Combining the estimates (4.3)–(4.8) completes the proof of (4.2). □

Remark 4.4 We prove (4.2) for arbitrary order of Lagrange elements, although we will only consider the case of linear element and quadratic element.

Lemma 4.3 gives the following error estimate on the whole domain.

Lemma 4.5 Given $u \in H^{r+2}(\Omega)$, we have

$$\|G_h I_h^r u - \nabla u\|_{0,\Omega} \lesssim h^{r+1} \|u\|_{r+2,\Omega}. \tag{4.9}$$

Proof Notice that

$$\begin{aligned} \|G_h I_h^r u - \nabla u\|_{0,\Omega}^2 &= \sum_{\tau \in \mathcal{T}_h} \|G_h I_h^r u - \nabla u\|_{0,\tau}^2 \\ &\lesssim \sum_{\tau \in \mathcal{T}_h} h^{2r+2} \|u\|_{r+2,\mathcal{K}_\tau}^2 \\ &\lesssim h^{2r+2} \|u\|_{r+2,\Omega}^2, \end{aligned}$$

where we have used Lemma 4.3 in the derivation of the the first inequality. Taking square root on both side gives (4.9). □

Now we are ready to present our main superconvergence result.

Theorem 4.6 *Let u be exact solution to the wave equation (2.11)–(2.13) and u_h be solution of the semi-discrete Galerkin finite element approximation (2.14)–(2.16). Suppose the mesh \mathcal{T}_h satisfies Condition(α). In addition assume $u \in L^\infty(0, T; H^{r+2}(\Omega))$, $\frac{\partial u}{\partial t} \in L^2(0, T; H^{r+2}(\Omega))$, and $\frac{\partial^2 u}{\partial t^2} \in L^2(0, T; H^{r+1}(\Omega))$, then for any $t \in (0, T]$, we have*

$$\|G_h u_h(\cdot, t) - \nabla u(\cdot, t)\|_{0,\Omega} \leq C(h^{r+\min(1,\alpha)} k^{r+3} + h^{r+1} k^{r+1}), \tag{4.10}$$

where C is a constant independent of k and h .

Proof We give the proof as in [1, 44]. Decompose $\|G_h u_h(\cdot, t) - \nabla u(\cdot, t)\|_{0,\Omega}$ in the following way:

$$\begin{aligned} &\|G_h u_h(\cdot, t) - \nabla u(\cdot, t)\|_{0,\Omega} \\ &= \|G_h u_h(\cdot, t) - G_h I_h^r u_h(\cdot, t) + G_h I_h^r u_h(\cdot, t) - \nabla u(\cdot, t)\|_{0,\Omega} \\ &\leq \|G_h u_h(\cdot, t) - G_h I_h^r u_h(\cdot, t)\|_{0,\Omega} + \|G_h I_h^r u_h(\cdot, t) - \nabla u(\cdot, t)\|_{0,\Omega} \\ &:= I_1 + I_2. \end{aligned} \tag{4.11}$$

According to Theorem 3.3, I_1 is bounded by $(h^{r+\min(1,\alpha)} k^{r+3} + h^{r+\min(1,\alpha)} k^{r+1})$. Lemma 4.5 implies that

$$\begin{aligned} I_2 &\leq \|G_h I_h^r u(\cdot, t) - \nabla u(\cdot, t)\|_{0,\Omega} \\ &\leq C h^{r+1} \|u(\cdot, t)\|_{r+2,\Omega} \\ &\leq C h^{r+1} \|u\|_{L^\infty(0,T;H^{r+2}(\Omega))} \\ &\leq C h^{r+1} k^{k+2}. \end{aligned}$$

Our proof is completed by combining the bound of I_1 and I_2 . □

Remark 4.7 We decompose $\|G_h u_h - \nabla u\|_{0,\Omega}$ into two parts $\|G_h u_h - G_h I_h^r u\|_{0,\Omega}$ and $\|G_h I_h^r u - \nabla u\|_{0,\Omega}$. However, $\|G_h u_h - G_h I_h^r u\|_{0,\Omega} \lesssim \|\nabla u_h - \nabla I_h^r u\|_{0,\Omega}$. As indicated in Remark 3.5, the error estimate (3.6) is not sharp with respect to k and hence the error estimate (4.10) is not sharp with respect to k .

5 Numerical Experiment

In the section, we present several numerical examples including both low and high frequencies to illustrate the superconvergence theory established in previous sections. In all the following numerical examples, we take time step as approximately a quarter of the space size, i.e., $\delta t \approx 0.25h$.

5.1 Numerical Results for Linear Element

In this subsection, we consider Σ to be an identity matrix $I_{2 \times 2}$ in (2.1), with the following initial conditions,

$$u(x, 0) = \sin(\pi x_1) \sin(\pi x_2), \quad x \in \Omega,$$

$$\frac{\partial u}{\partial t}(x, 0) = -\sin(\pi x_1) \sin(\pi x_2), \quad x \in \Omega,$$

and f is chosen to fit the exact solution $u(x, t) = e^{-t} \sin(\pi x_1) \sin(\pi x_2)$ and $\Omega = [0, 1] \times [0, 1]$.

In order to obtain superconvergence results of linear element, we consider an unconditionally stable second order accurate time discretization. Let N be a positive integer and define the time step as

$$\delta t = \frac{T}{N}, \quad t^n = n\delta t, \quad n = 0, 1, \dots, N. \tag{5.1}$$

For any function w , the value of w at time t^n is denoted by w^n . We also introduce the following notation

$$w^{n+1/2} = \frac{w^{n+1} + w^n}{2}, \quad w^{n,1/4} = \frac{w^{n+1} + 2w^n + w^{n-1}}{4},$$

$$\partial_t w^{n+1/2} = \frac{w^{n+1} - w^n}{\delta t}, \quad \partial_t w^n = \frac{w^{n+1} - w^{n-1}}{2\delta t},$$

$$\partial_{tt} w^n = \frac{w^{n+1} - 2w^n + w^{n-1}}{\delta t^2}.$$
(5.2)

We consider the following full discrete Galerkin approximation [16] of linear element, i.e., to find a sequence $\{u_h^n\}_{n=1}^N \in S^{h,1}$ such that

$$(\partial_{tt} u_h^n, v_h) + a(u_h^{n,1/4}, v_h) = (f^{n,1/4}, v_h), \quad \forall v_h \in S^{h,1}. \tag{5.3}$$

Note the above scheme needs initial conditions of two time steps. As in [41], we consider Taylor expansion of u at $t = 0$,

$$u(x, \delta t) = u(x, 0) + \delta t \frac{\partial u}{\partial t}(x, 0) + \frac{\delta t^2}{2} \frac{\partial^2 u}{\partial t^2}(x, 0) + \frac{\delta t^3}{6} \frac{\partial^3 u}{\partial t^3}(x, 0) + O(\delta t^4),$$

and replace the higher derivatives of t by derivatives of x using (2.1), which yields the following initial conditions,

$$u_h^0 = I_h^1 u_0,$$

$$u_h^1 = I_h^1 u_h^0 + \delta t I_h^1 q_0 + \frac{\delta t^2}{2} I_h^1 (\Delta u_0 + I_h^1 f(x, 0)) + \frac{\delta t^3}{6} I_h^1 (\Delta q_0 + \frac{\partial f}{\partial t}(x, 0)),$$

with u_0 and q_0 given in (2.2).

Table 1 shows the numerical errors at the final computational time $T = 1$ on regular pattern uniform mesh. As we expected, $\|\nabla u - \nabla u_h\|_{0,\Omega}$ decays at the optimal rate of $O(h)$. $\|\nabla u_h - \nabla I_h^1 u\|_{0,\Omega}$ and $\|\nabla u_h - G_h u_h\|_{0,\Omega}$ both converge at the superconvergence rate of $O(h^2)$, which is consistent with our theoretical results in Theorems 3.3 and 4.6, respectively. We test on chevron pattern uniform mesh and its numerical errors are displayed in Table 2, which is similar to regular pattern uniform mesh.

Next, we turn to Criss-cross pattern uniform mesh and we list its numerical errors in Table 3. Different from the previous two types of uniform meshes, this mesh pattern doesn't satisfy

Table 1 Numerical results of linear element case on regular pattern uniform mesh

Dof	$\ \nabla u - \nabla u_h\ _{0,\Omega}$	order	$\ \nabla u_h - \nabla I_h^1 u\ _{0,\Omega}$	order	$\ \nabla u_h - G_h u_h\ _{0,\Omega}$	order
289	8.009e-02	–	3.052e-03	–	1.738e-02	–
1089	4.010e-02	0.52	7.712e-04	1.04	4.585e-03	1.00
4225	2.006e-02	0.51	1.960e-04	1.01	1.174e-03	1.00
16641	1.003e-02	0.51	4.950e-05	1.00	2.968e-04	1.00
66049	5.014e-03	0.50	1.244e-05	1.00	7.459e-05	1.00

Table 2 Numerical results of linear element on chevron pattern uniform mesh

Dof	$\ \nabla u - \nabla u_h\ _{0,\Omega}$	order	$\ \nabla u_h - \nabla I_h^1 u\ _{0,\Omega}$	order	$\ \nabla u_h - G_h u_h\ _{0,\Omega}$	order
289	8.019e-02	–	5.709e-03	–	1.224e-02	–
1089	4.019e-02	0.52	3.664e-03	0.33	3.170e-03	1.02
4225	2.007e-02	0.51	5.708e-04	1.37	8.084e-04	1.01
16641	1.003e-02	0.51	1.348e-04	1.05	2.038e-04	1.01
66049	5.014e-03	0.50	1.642e-05	1.53	5.114e-05	1.00

Table 3 Numerical results of linear element on Criss-cross pattern uniform mesh

Dof	$\ \nabla u - \nabla u_h\ _{0,\Omega}$	order	$\ \nabla u_h - \nabla I_h^1 u\ _{0,\Omega}$	order	$\ \nabla u_h - G_h u_h\ _{0,\Omega}$	order
545	6.238e-02	–	6.471e-02	–	8.723e-03	–
2113	3.735e-02	0.38	2.135e-02	0.82	1.361e-03	1.37
8321	2.275e-02	0.36	1.542e-02	0.24	3.380e-04	1.02
33025	1.427e-02	0.34	1.089e-02	0.25	8.180e-05	1.03
131585	7.877e-03	0.43	6.239e-03	0.40	2.006e-05	1.02

Condition (α) and thus there is no supercloseness between the gradient of finite element solution and the gradient of interpolation of exact solution; see the fifth column of Table 3. However, even in this case, our results still show the superconvergent of gradient at the rate of $O(h^2)$; see the seventh column of Table 3. In fact, we also tested Union-Jack pattern uniform mesh, but did not present the numerical results here due to the similarity to the results by using Criss-cross pattern uniform mesh.

At the end, we consider unstructured meshes. We start from an initial mesh generated by EasyMesh [33] followed by four levels of uniform refinement. Table 4 shows the supercloseness and superconvergence of recovered gradient.

5.2 Numerical Results for Quadratic Element

In this subsection, we consider (2.1) with $\Sigma = I_{2 \times 2}$ that has a traveling wave solution as in [10]. The domain is chosen as $\Omega = [0, 2] \times [0, 2]$, and the initial conditions and boundary conditions are given by the exact solution

$$u(x, t) = \cos(\sqrt{2}\pi t + \pi x_1) \cos(\pi x_2).$$

Table 4 Numerical results of linear element on Delaunay mesh

Dof	$\ \nabla u - \nabla u_h\ _{0,\Omega}$	order	$\ \nabla u_h - \nabla I_h^1 u\ _{0,\Omega}$	order	$\ \nabla u_h - G_h u_h\ _{0,\Omega}$	order
513	4.567e-02	–	7.868e-03	–	7.587e-03	–
1969	2.266e-02	0.52	2.137e-03	0.97	2.122e-03	0.95
7713	1.131e-02	0.51	5.686e-04	0.97	5.782e-04	0.95
30529	5.651e-03	0.50	1.486e-04	0.98	1.529e-04	0.97
121473	2.825e-03	0.50	3.904e-05	0.97	4.030e-05	0.97

To get superconvergence of quadratic element, one needs higher order time discretization, and thus we choose the fourth order time discretization used in [10,35] which can be reformulated into a predictor–corrector form. The second-order predictor step is

$$\left(\frac{u_h^* - 2u_h^n + u_h^{n-1}}{\delta t^2}, w_h \right) = -(\nabla u_h^n, \nabla w_h), \quad w_h \in S_h^r; \tag{5.4}$$

and the corrector step is

$$v_h = \frac{u_h^* - 2u_h^n + u_h^{n-1}}{\delta t^2}, \tag{5.5}$$

$$(u_h^{n+1}, w_h) = (u_h^*, w_h) - \frac{\delta t^4}{12} (\nabla v_h, \nabla w_h), \quad w_h \in S_h^r. \tag{5.6}$$

In the following, we compute the numerical error at time $T = 1$. Table 5 lists the numerical results for quadratic element on regular pattern uniform mesh. Consistent with Theorems 3.3 and 4.6, the convergence rate of $O(h^3)$ is observed for $\|\nabla u_h - \nabla I_h^2 u\|_{0,\Omega}$ and $\|\nabla u_h - G_h u_h\|_{0,\Omega}$.

Table 6 shows the convergence of numerical errors for quadratic element on the same Delaunay mesh as in Example 1, from which one can clearly observe desired supercloseness results and superconvergence results.

5.3 Numerical Results for High-Frequency Wave Propagation

In this subsection, we consider (2.1) with $\Sigma = I_{2 \times 2}$, and the high-frequency WKB initial conditions,

$$\begin{cases} u_0(x) = A_0(x)e^{ikS_0(x)}, \\ \partial_t u_0(x) = k B_0(x)e^{ikS_0(x)}. \end{cases}$$

Table 5 Numerical results of quadratic element on regular pattern mesh

Dof	$\ \nabla u - \nabla u_h\ _{0,\Omega}$	order	$\ \nabla u_h - \nabla I_h^1 u\ _{0,\Omega}$	order	$\ \nabla u_h - G_h u_h\ _{0,\Omega}$	order
1089	6.697e-02	–	8.972e-03	–	1.370e-02	–
4225	1.686e-02	1.04	1.155e-03	1.55	1.191e-03	1.84
16641	4.220e-03	1.02	1.467e-04	1.52	1.136e-04	1.73
66049	1.055e-03	1.01	1.598e-05	1.62	1.188e-05	1.65
263169	2.639e-04	1.01	2.334e-06	1.40	1.340e-06	1.58

Table 6 Numerical results of quadratic element on Delaunay mesh

Dof	$\ \nabla u - \nabla u_h\ _{0,\Omega}$	order	$\ \nabla u_h - \nabla I_h^1 u\ _{0,\Omega}$	order	$\ \nabla u_h - G_h u_h\ _{0,\Omega}$	order
1969	2.408e-02	–	2.347e-03	–	3.480e-03	–
7713	6.033e-03	1.03	4.043e-04	1.31	3.365e-04	1.74
30529	1.509e-03	1.01	7.084e-05	1.28	3.493e-05	1.66
121473	3.775e-04	1.01	1.247e-05	1.26	4.005e-06	1.57
484609	9.439e-05	1.00	2.195e-06	1.26	5.148e-07	1.49

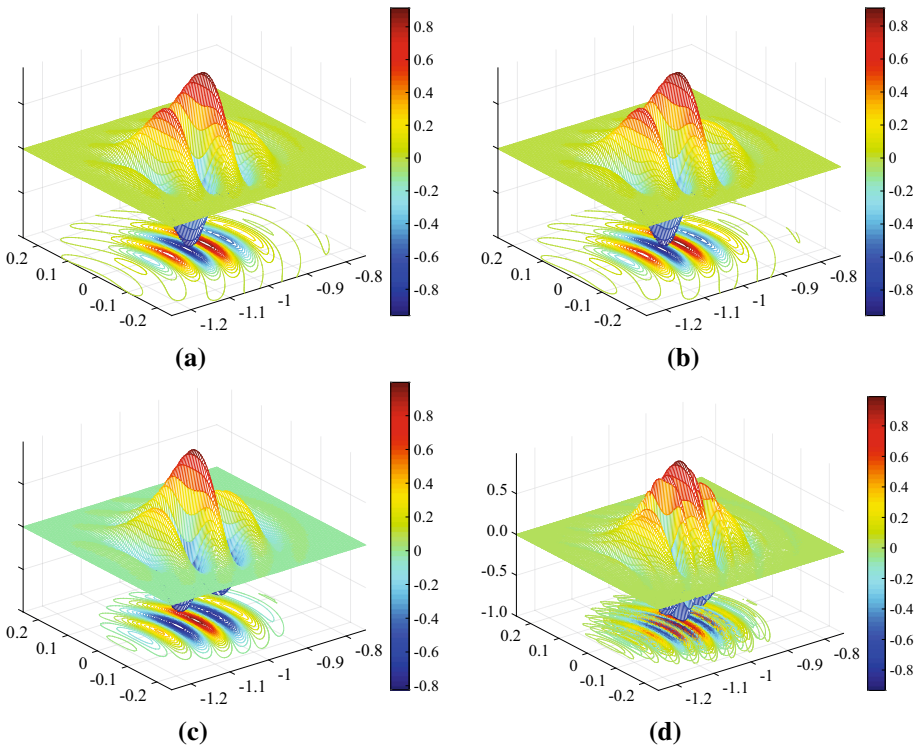


Fig. 1 Plot of high frequency wave when wave number $k = 64$ when mesh size $h = 2^{-10}$. **a** Real part of exact solution. **b** Real part of numerical solution. **c** Imaginary part of exact solution. **d** Imaginary part of numerical solution

We chose f, A_0, B_0, S_0 to fit the exact solution,

$$u = \exp(-100((x + t)^2 + y^2)) \exp(ik(-x + \cos(2y) + 5t)). \tag{5.7}$$

We compute the numerical solution to (2.1) at time $t = 1$. The computational domain is $[-1.5, 0.5] \times [-1, 1]$. The mesh \mathcal{T}_h is obtained by first dividing the computation domain Ω into $N \times N$ squares and then dividing every square into two right triangles. Let u_h be the linear finite element solution on a mesh \mathcal{T}_h at time $T = 1$. The number of degree of freedom

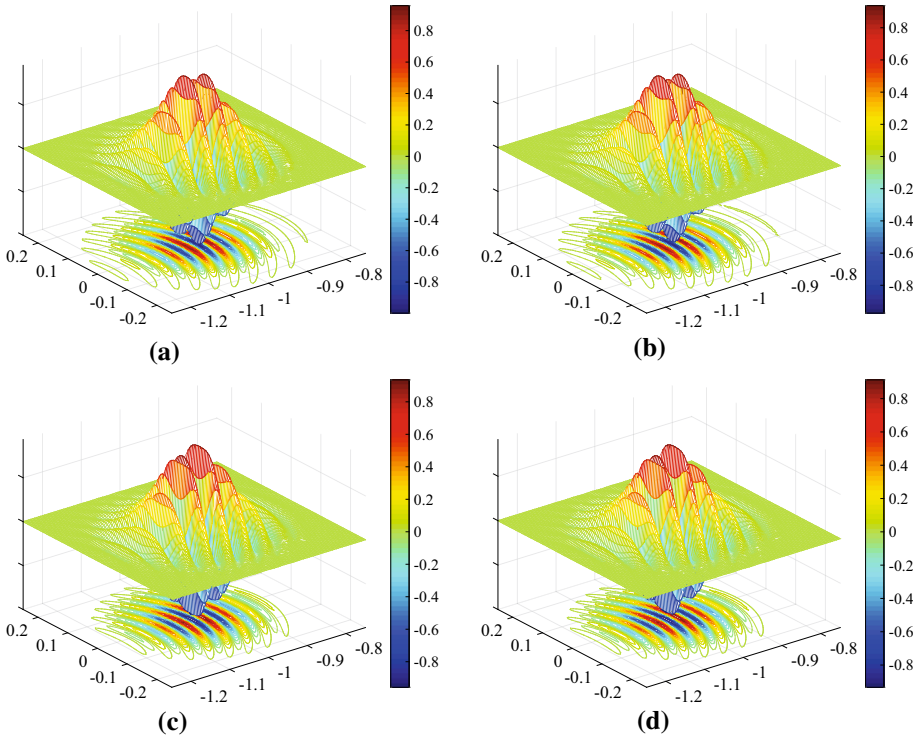


Fig. 2 Plot of high frequency wave when wave number $k = 128$ when mesh size $h = 2^{-10}$. **a** Real part of exact solution. **b** Real part of numerical solution. **c** Imagary part of exact solution. **d** Imagary part of numerical solution

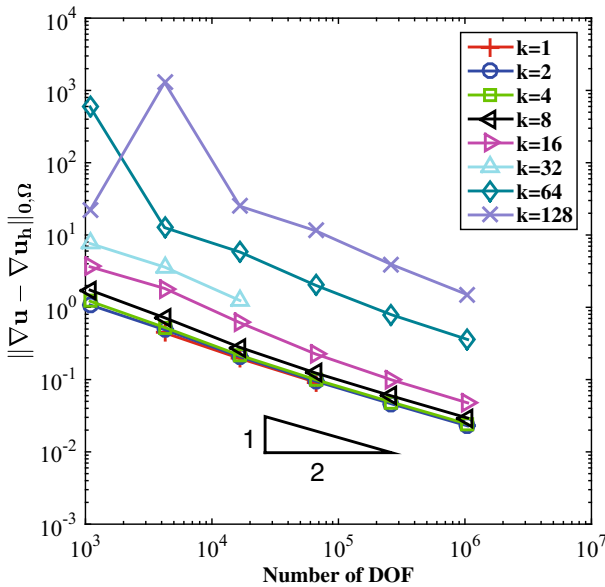


Fig. 3 Plot of $\|\nabla u - \nabla u_h\|_{0,\Omega}$ with respect to h

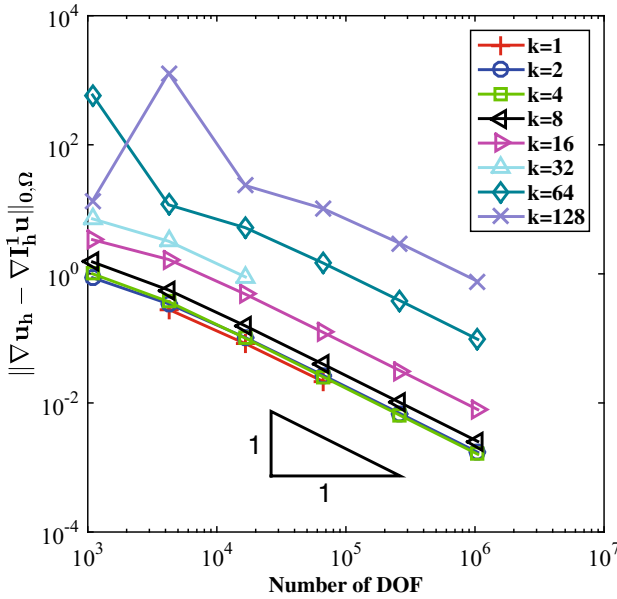


Fig. 4 Plot of $\|\nabla u_h - \nabla I_h^1 u\|_{0,\Omega}$ with respect to h

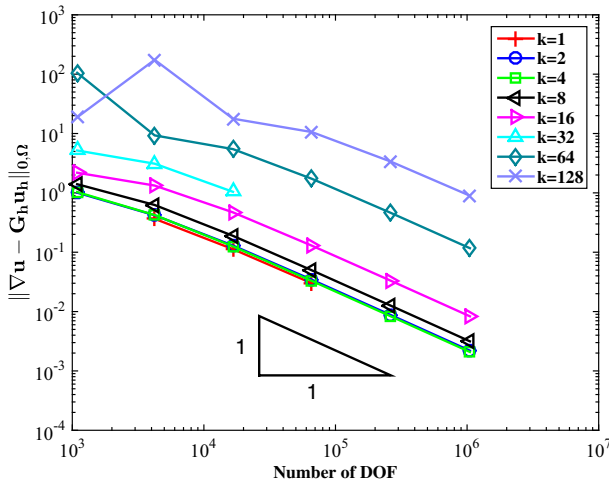


Fig. 5 Plot of $\|\nabla u - G_h u_h\|_{0,\Omega}$ with respect to h

is $(N + 1)^2$ and mesh size is $h = \frac{2}{N}$. Here we take $N = 2^j$ with $j = 6, 7, 8, 9, 10$. Note that in this case $\alpha = 1$. In the following, we compute for both low-frequency and high-frequency wave. Specifically, we choose $k = 2^j$, with $j = 0, 1, 2, 3, 4, 5, 6, 7$.

At initial time $t = 0$, the wave packet is localized at the point $(0, 0)$. At $t = 1$, the wave packet propagates to the point $(-1, 0)$. As one can observe from (5.7), there would be high-frequency oscillations in the solutions of large k . To illustrate this, we graph the real and imaginary part of the exact solutions on the small domain $[-1.25, 0.75] \times [-0.25, 0.25]$ for

Table 7 Results of high frequency wave when $k = 64$

Dof	$\ \nabla u - \nabla u_h\ _{0,\Omega}$	order	$\ \nabla u_h - \nabla I_h^1 u\ _{0,\Omega}$	order	$\ \nabla u_h - G_h u_h\ _{0,\Omega}$	order
4225	2.599e+01	–	2.556e+01	–	1.390e+01	–
16641	7.874e+00	0.87	7.425e+00	0.90	6.661e+00	0.54
66049	2.433e+00	0.85	2.013e+00	0.95	2.154e+00	0.82
263169	8.593e–01	0.75	5.139e–01	0.99	5.773e–01	0.95
1050625	3.682e–01	0.61	1.286e–01	1.00	1.459e–01	0.99

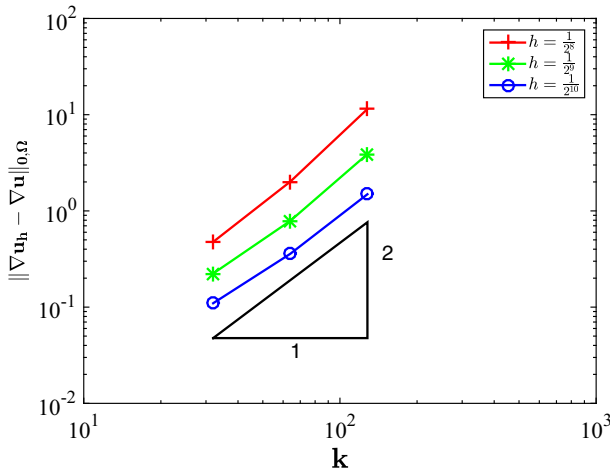


Fig. 6 Plot of $\|\nabla u - \nabla u_h\|_{0,\Omega}$ with respect to k

$k = 64$ and $k = 128$, see Figs. 1a, c and 2a, c. We also plot the real and imaginary part of numerical solutions on the finest mesh \mathcal{T}_h with $h = 2^{-10}$ for $k = 64$ and $k = 128$. One can see that the numerical solutions match well with the exact solutions.

Figure 3 plots H_1 -semi error of finite element solution for different numbers of degree of freedoms. For low frequency wave ($k = 1, 2, 4, 8, 16$), it shows optimal convergence rate. For high frequency wave ($k = 32, 64, 128$), it requires the mesh size small enough to converge optimally at the rate of $O(h)$.

Figure 4 shows the supercloseness between finite element solution and the interpolation of exact solution. Similar to H_1 -semi error of finite element solution, it shows the order of $O(h^2)$ supercloseness results for both cases of low-frequency and high-frequency waves. Figure 5 shows the numerical error of recovered gradient, in which the order of $O(h^2)$ superconvergent rate can be observed. Table 7 gives the numerical results for the case $k = 64$, in which one can notice that the errors of recovered gradient are smaller than the errors of gradient of finite element solution even in coarse meshes.

To see clearly the dependence of errors on k , we plot the above three errors with respect to k on the same mesh \mathcal{T}_h , see Figs. 6, 7 and 8. It shows that $\|\nabla u - \nabla u_h\|_{0,\Omega}$ depends on k^2 while $\|\nabla u_h - \nabla I_h^1 u\|_{0,\Omega}$ and $\|G_h u_h - \nabla u\|_{0,\Omega}$ depend on k^3 . It means our error estimates may not be sharp with respect to k as we comment in Remarks 2.5, 3.5 and 4.7.

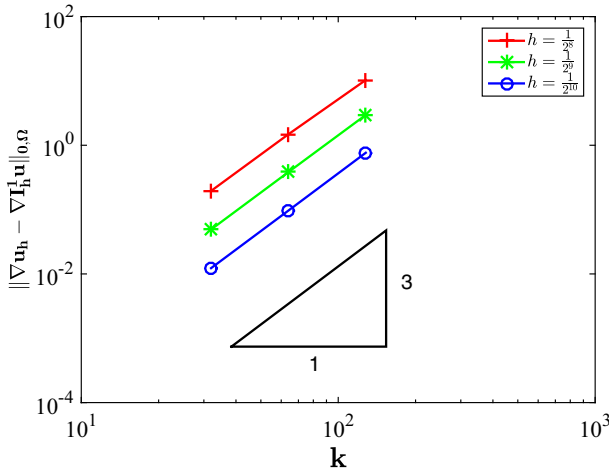


Fig. 7 Plot of $\|\nabla u_h - \nabla I_h^1 u\|_{0,\Omega}$ with respect to k

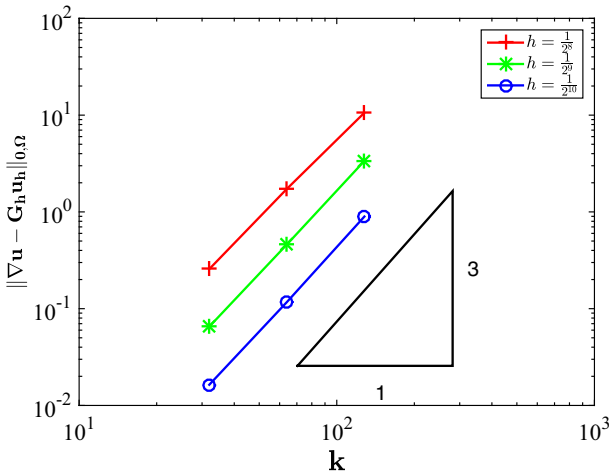


Fig. 8 Plot of $\|\nabla u - G_h u_h\|_{0,\Omega}$ with respect to k

6 Conclusion

In this paper, we generalized the polynomial preserving recovery (PPR) method to compute wave propagation of high-frequency. Specifically, we analyzed the supercloseness of finite element solution and interpolation solution with explicit dependence on wave frequency k , and proved the superconvergence of PPR for wave equation. Numerical results were given in both low frequency and high frequency to confirm our theoretic results, which indicated the sharpness of theoretical results with respect to h . The purpose of PPR is not only to improve the gradient approximation but also to serve as an asymptotically exact a posteriori error estimator for wave propagation. One may notice that, Theorem 4.6 implies that one needs at least a mesh size of order $o(k)$ to have an accurate approximation which might be still computationally expensive in high dimensional cases. In future, we plan to relax this

mesh-size restriction by including high-frequency elements (e.g. high-frequency plane waves or complex Gaussian functions) in the finite element method as in the tailored finite point method and frozen Gaussian approximation [24,43].

References

1. Ainsworth, M., Oden, J.: *A Posteriori Error Estimation in Finite Element Analysis*. Wiley, New York (2000)
2. Babuška, I., Strouboulis, T., Upadhyay, C.S., Gangaraj, S.K., Copps, K.: Validation of a posteriori error estimators by numerical approach. *Int. J. Numer. Methods Eng.* **37**(7), 1073–1123 (1994)
3. Baccouch, M.: A superconvergent local discontinuous Galerkin method for the second-order wave equation on Cartesian grids. *Comput. Math. Appl.* **68**(10), 1250–1278 (2014)
4. Baker, G.A.: Error estimates for finite element methods for second order hyperbolic equations. *SIAM J. Numer. Anal.* **13**(4), 564–576 (1976)
5. Bank, R., Xu, J.: Asymptotically exact a posteriori error estimators. I. Grids with superconvergence. *SIAM J. Numer. Anal.* **41**(6), 2294–2312 (2003). (Electronic)
6. Brenner, S.C., Scott, L.R.: *The mathematical theory of finite element methods*, 3rd edn. In: *Texts in Applied Mathematics*, vol. 15. Springer, New York (2008)
7. Carstensen, C., Bartels, S.: Each averaging technique yields reliable a posteriori error control in FEM on unstructured grids. I. Low order conforming, nonconforming, and mixed FEM. *Math. Comput.* **71**(239), 945–969 (2002). (Electronic)
8. Chen, C., Hu, S.: The highest order superconvergence for bi-k degree rectangular elements at nodes: a proof of 2k-conjecture. *Math. Comput.* **82**(283), 1337–1355 (2013)
9. Chen, L., Xu, J.: A posteriori error estimator by post-processing. In: Tang, T., Xu, J. (eds.) *Adaptive Computations: Theory and Algorithms*. Science Press, Beijing (2006)
10. Chou, C.-S., Shu, C.-W., Xing, Y.: Optimal energy conserving local discontinuous Galerkin methods for second-order wave equation in heterogeneous media. *J. Comput. Phys.* **272**, 88–107 (2014)
11. Ciarlet, P.G.: *The Finite Element Method for Elliptic Problems*. North-Holland, Amsterdam (1978)
12. Cockburn, B., Quennesson, V.: Uniform-in-time superconvergence of the HDG methods for the acoustic wave equation. *Math. Comput.* **83**(285), 65–85 (2014)
13. Douglas, J. Jr., Dupont, T.: Some superconvergence results for Galerkin methods for the approximate solution of two-point boundary problems. In: *Topics in Numerical Analysis (Proc. Roy. Irish Acad. Conf., University Coll., Dublin, 1972)*, pp. 89–92. Academic Press, London (1973)
14. Douglas, J., Dupont, T.: Galerkin approximations for the two point boundary problem using continuous, piecewise polynomial spaces. *Numer. Math.* **22**, 99–109 (1974)
15. Dougalis, V.A., Serbin, S.M.: On the superconvergence of Galerkin approximations to second-order hyperbolic equations. *SIAM J. Numer. Anal.* **17**(3), 431–446 (1980)
16. Dupont, T.: L^2 -estimates for Galerkin methods for second order hyperbolic equations. *SIAM J. Numer. Anal.* **10**, 880–889 (1973)
17. Evans, L.C.: *Partial Differential Equations*, 2nd edn. American Mathematical Society, Providence (2010)
18. Formaggia, L., Perotto, S.: New anisotropic a priori error estimates. *Numer. Math.* **89**(4), 641–667 (2001)
19. Formaggia, L., Perotto, S.: Anisotropic error estimates for elliptic problems. *Numer. Math.* **94**(1), 67–92 (2003)
20. Guo, H., Zhang, Z.: Gradient recovery for the Crouzeix–Raviart element. *J. Sci. Comput.* **64**(2), 456–476 (2015)
21. Guo, H., Zhang, Z., Zhao, R.: Superconvergent Two-grid Methods For Elliptic Eigenvalue Problems, *J Sci Comput*, 1–24 , (2016). doi:[10.1007/s10915-016-0245-2](https://doi.org/10.1007/s10915-016-0245-2)
22. Huang, W., Russell, R.: *Adaptive Moving Mesh Methods*, Applied Mathematical Sciences, 174. Springer, New York (2011)
23. Huang, Y., Xu, J.: Superconvergence of quadratic finite elements on mildly structured grids. *Math. Comput.* **77**(263), 1253–1268 (2008)
24. Huang, Z.Y., Yang, X.: Tailored finite point method for first order wave equation. *J. Sci. Comput.* **49**(3), 351–366 (2011)
25. Lakhany, A.M., Marek, I., Whiteman, J.R.: Superconvergence results on mildly structured triangulations. *Comput. Methods Appl. Mech. Eng.* **189**(1), 1–75 (2000)
26. Ihlenburg, F., Babuška, I.: Finite element solution of the Helmholtz equation with high wave number. I. The h-version of the FEM. *Comput. Math. Appl.* **30**(9), 9–37 (1995)

27. Ihlenburg, F., Babuška, I.: Finite element solution of the Helmholtz equation with high wave number. II. The h-p version of the FEM. *SIAM J. Numer. Anal.* **34**(1), 315–358 (1997)
28. Lin, Q., Wang, H., Lin, T.: Interpolated finite element methods for second order hyperbolic equations and their global superconvergence. *Syst. Sci. Math. Sci.* **6**(4), 331–340 (1993)
29. Lions, J.-L., Magenes, E.: *Non-homogeneous Boundary Value Problems and Applications*, vol. I. Springer, New York (1972)
30. Naga, A., Zhang, Z.: A posteriori error estimates based on the polynomial preserving recovery. *SIAM J. Numer. Anal.* **42**(4), 1780–1800 (2004). (Electronic)
31. Naga, A., Zhang, Z.: The polynomial-preserving recovery for higher order finite element methods in 2D and 3D. *Discrete Contin. Dyn. Syst. Ser. B* **5**(3), 769–798 (2005)
32. Naga, A., Zhang, Z., Zhou, A.: Enhancing eigenvalue approximation by gradient recovery. *SIAM J. Sci. Comput.* **28**(4), 1289–1300 (2006). (Electronic)
33. B. Niceno, *EasyMesh Version 1.4: A Two-Dimensional Quality Mesh Generator*, <http://www.dinma.univ.trieste.it/nirftc/research/easymesh>
34. Shi, D., Li, Z.: Superconvergence analysis of the finite element method for nonlinear hyperbolic equations with nonlinear boundary condition. *Appl. Math. J. Chin. Univ. Ser. B* **23**(4), 455–462 (2008)
35. Sjögreen, B., Petersson, N.A.: A fourth order accurate finite difference scheme for the elastic wave equation in second order formulation. *J. Sci. Comput.* **52**(1), 17–48 (2012)
36. Wahlbin, L.: Superconvergence in Galerkin finite element methods. *Lecture Notes in Mathematics*, vol. 1605. Springer, Berlin (1995)
37. Wang, F., Chen, Y., Tang, Y.: Superconvergence of fully discrete splitting positive definite mixed FEM for hyperbolic equations. *Numer. Methods Partial Differ. Equ.* **30**(1), 175–186 (2014)
38. Wu, H.: Pre-asymptotic error analysis of CIP-FEM and FEM for the Helmholtz equation with high wave number. Part I: linear version. *IMA J. Numer. Anal.* **34**(3), 1266–1288 (2014)
39. Wu, H., Zhang, Z.: Can we have superconvergent gradient recovery under adaptive meshes? *SIAM J. Numer. Anal.* **45**(4), 1701–1722 (2007)
40. Wu, H., Zhang, Z.: Enhancing eigenvalue approximation by gradient recovery on adaptive meshes. *IMA J. Numer. Anal.* **29**(4), 1008–1022 (2009)
41. Xing, Y., Chou, C.-S., Shu, C.-W.: Energy conserving local discontinuous Galerkin methods for wave propagation problems. *Inverse Probl. Imaging* **7**(3), 967–986 (2013)
42. Xu, J., Zhang, Z.: Analysis of recovery type a posteriori error estimators for mildly structured grids. *Math. Comput.* **73**(247), 1139–1152 (2004). (Electronic)
43. Lu, J., Yang, X.: Frozen Gaussian approximation for high frequency wave propagation. *Commun. Math. Sci.* **9**(3), 663–683 (2011)
44. Zhang, Z., Naga, A.: A new finite element gradient recovery method: superconvergence property. *SIAM J. Sci. Comput.* **26**(4), 1192–1213 (2005). (Electronic)
45. Zienkiewicz, O.C., Zhu, J.Z.: A simple error estimator and adaptive procedure for practical engineering analysis. *Int. J. Numer. Methods Eng.* **24**, 337–357 (1987)
46. Zienkiewicz, O.C., Zhu, J.Z.: The superconvergent patch recovery and a posteriori error estimates. I. The recovery technique. *Int. J. Numer. Methods Eng.* **33**, 1331–1364 (1992)
47. Zienkiewicz, O.C., Zhu, J.Z.: The superconvergent patch recovery and a posteriori error estimates. II. Error estimates and adaptivity. *Int. J. Numer. Methods Eng.* **33**, 1331–1364 (1992)